UDC 616.894-053.8:612.314

N. A. GHAZARYAN,[1] K. V. SIMONYAN[1], M. H. DANIELYAN[1],
N. A. ZAKARYAN[1], L. A. GHULIKYAN[1], G. R. KIRAKOSYAN[1],
V. A. CHAVUSHYAN[1], and N. M. AYVAZYAN[1]

NEUROPROTECTIVE EFFECTS OF *MACROVIPERA LEBETINA* SNAKE VENOM IN THE MODEL OF ALZHEIMER'S DISEASE

Received February 22, 2016

Pathological features of Alzheimer's disease (AD) include accumulation and deposition of β-amyloid (Aβ) in the brain, activation of astrocytes and microglia, and disruption of cholinergic neurotransmission. In our experiments on rats, a model of AD was created by intracerebroventricular (i.c.v.) injections of $A\beta_{25–35}$ amyloid. In another animal group, this was combined with intramuscular (i.m.) injections of small doses of *Macrovipera lebetina* (ML) snake venom (50 μl of 5% solution of an LD_{50} dose per animal seven times with one-day-long intervals). In the AD model, the most vulnerable neurons were found in the hippocampal fields CA1 and CA3. The phosphatase activity in the hippocampus of Aβ-injected rats sharply dropped. Systemic administration of small doses of ML venom induced positive changes in the structural characteristics of hippocampal neurons, increased the density of neurons in the above fields, normalized metabolism, and intensified Ca^{2+}-dependent phosphorylation. Under the action of ML venom, the proportion of responses of hippocampal pyramidal neurons after high-frequency tetanic stimulation of the ipsilateral entorhinal cortex in the form of tetanic depression- posttetanic potentiation increased, and an overall increase in the firing rate of hippocampal neurons was observed. The intensity of free radical processes in some tissues of Aβ-affected animals became much lower under the action of ML venom. Thus, small doses of this venom manifest clear neuroprotective effects in the rat AD model.

Keywords: Alzheimer's disease, Aβ-induced neurodegeneration, hippocampus, *Macrovipera lebetina* venom, Ca^{2+}-dependent acid phosphatase.

INTRODUCTION

According to current statistics based on modern diagnostic approaches, Alzheimer's disease has been proved to be one of the most progressing diseases in the world and is on a top of the respective statistical sequence after cardiovascular diseases and cancer. Alzheimer's disease is a neurodegenerative disorder characterized by slow development, progressing deterioration of memory and intelligence, and specific symptoms often combined with normal senile symptoms [1]. The disease is frequently detected at a relatively young age, with a clear deterioration of initial symptoms of the olfactory perception and spatial disorientation. Loss of neurons forming cortico-cortical projections in the associative neocortex emerges as the pathological outcome most directly related to dementia observed in AD [2]. It is generally believed that one of the main causes of Alzheimer's disease is accumulation of neurotoxic β-amyloid peptide (Aβ) in the brain [3, 4]. Alzheimer's disease induces a deficiency of acetylcholine in the hippocampus due to abnormal activation of cholinesterase [5, 6]. Hyperproduction of free radicals is supposed to be a significant factor playing an important role in the pathogenesis of this disease.

Several groups of drugs were proposed for the treatment of Alzheimer's disease to date. These include antioxidants, inhibitors of acetylcholinesterase, drugs affecting glutamate receptors, agents preventing the formation of β-amyloid accumulations and neurofibrillary tangles, anti-inflammatory agents, and others. The effects of some snake venoms (of both *Elapidae* and *Viperidae*) on synaptic transmission have been intensely studied from this spect. There are

[1] Laboratory of Toxicology and Molecular Systematics, Orbeli Institute of Physiology of the NAS of RA, Yerevan, Armenia.
Correspondence should be addressed to N. A. Ghazaryan (e-mail: naringhazaryan@gmail.com).

reports describing the influences of snake venom on cholinergic neurons [7–9].

Macrovipera lebetina, ML (gurza, giurza, Levantine viper) is known as a rather dangerous snake. In Armenia, its subspecies, *Macrovipera lebetina obtuza*, is the most important poisonous snake [10]. A specific toxin has not been identified in the venom of this snake; the latter has no real toxins in its venom similar to three-finger toxins of *Elapidae*. The ML venom components form complexes with other non-enzymatic proteins, and this provides the high toxic efficiency through synergy (like ammoditoxin from *Vipera ammodites*, etc.) [11,12]. The proteins of ML venom belong to a few major protein families, including both enzymes (serine proteinases, Zn^{2+}-metalloproteinases, L-amino acid oxidase, group II PLA2) and also proteins with no enzymatic activity (disintegrins, C-type lectins, natriuretic peptides, myotoxins, CRISP toxins, nerve and vascular endothelium growth factors, cystein, and Kunitz-type proteinase inhibitors). Some proteins found in the ML venom are characteristic for only the above-mentioned subspecies (e.g., a short disintegrin, obtustatin) [13].

Our study aimed at assessing the effects of ML venom on some electrophysiological, morphological, and histochemical parameters in a rat model of Alzheimer's disease. Considering the possible role of free radicals of the pathogenesis of this disease, we also studied changes in the free radical oxidation processes in several tissues of the rats subjected to the action of β-amyloid.

METHODS

Animals. Adult male albino Wistar rats weighing 200 ± ± 30 g were purchased from the Experimental Center of the Orbeli Institute of Physiology (NAS RA) [14]. The animals were kept under standard vivarium conditions at 25 ± 2°C, 12/12 h light/dark cycle (lights on at 7.00), and with food and water *ad libitum*. The experiments were performed within the same time interval (9.00–12.00) in separate isolated laboratories that had the same environmental conditions as the colony room.

Five groups of animals were formed; these were

1) Intact group, rats subjected to no experimental interventions;

2) Group Aβ, rats injected intracerebroventricularly (i.c.v.) with $A\beta_{25–35}$ amyloid (Sigma-Aldrich, USA) according to Maurice et al. [15 ?? 16] in combination with intramuscular (i.m.) injections of 50 μl of sterile distilled water;

3) Group Aβ+venom, rats i.c.v. injected with $A\beta_{25–35}$ amyloid in combination with i.m. injections of ML venom (50 μl of 5% solution of an LD_{50} dose per animal seven times with one-day-long intervals). The LD_{50} of ML venom for mice (18.47 μg) has been measured previously [15];

4) Venom group, rats i.c.v. injected with distilled water and i.m. injected with the above dose of ML venom according to the above-mentioned scheme, and

5) Sham group, rats i.c.v. injected with distilled water and i.m. injected also with sterile distilled water.

Aggregation of $A\beta_{25–35}$ was performed as was described earlier [16, 17]. One mg of the peptide was dissolved in 1.0 ml of bidistilled water; the solution was then maintained in a temperature-regulated environment at 37°C for 3 days. The formation of amyloid fibrils was examined under a light microscope. Animals were i.c.v. treated with aggregated $A\beta_{25–35}$ at a dose of 2 μg/100 g body mass (0.5 μl of the solution at a rate of 1.0 μl/min) using a 10-μl Hamilton microsyringe with a 26G needle.

All experiments were performed in 16 weeks after $A\beta_{25–35}$ amyloid injections.

Histochemical Analysis. For histochemical investigation, parts of the brain were fixed for 2–3 days in 5% neutral formalin prepared on phosphate buffer (pH 7.4). The fixation was performed at 4°C for 48 h. Frontal frozen brain sections (50 to 60 μm thick) were prepared, washed in distilled water, and transferred to an incubation mixture for selective detection of nerve cells. This mixture included 20 ml of 0.38% lead acetate solution, 5 ml of 1.0 M acetate buffer (pH 5.6), and 5 ml of 2% solution of sodium β-glycerophosphate. Incubation was performed in a thermostat at 37°C for 1 to 3 h; then, sections were washed in distilled water, developed in a sodium sulfate solution, and, after repeated washings, were ready.

The sections were processed of detect the activity of Ca^{2+}-dependent acid phosphatase (AP) [18], a modification of the lead method [19], based on the ability of calcium ions to capture inorganic phosphate. Calcium phosphate is converted into lead phosphate, and, subsequently, into black/dark brown lead sulfide. The histochemical study was carried out after electrophysiological recording under analogous experimental conditions and on the same animal. This approach is based on the detection of intracellular

phosphorus-containing substrates playing a key role in metabolic energetic processes. Apart from its histochemical significance, the method allows experimenters to reveal clearly neurons and glial cells in the brain; thus, it demonstrates real advantages from the strictly histological aspect.

Electrophysiological Recordings. In acute experiments, the animals were anesthetized (Urethan, 1.2 g/kg), immobilized with 1% ditiline (25 mg/kg.i.p.), fixed in a stereotaxic apparatus, and begun to be artificially respirated. The spinal cord was transected at a T2–T3 level. Stereotaxically oriented glass microelectrodes (tip diameter 1–2 μm) were filled with 2.0 M NaCl and inserted into the hippocampal fields *CA1* and *CA3*, to record spike activity of single neurons evoked by high-frequency stimulation of the ipsilateral entorhinal cortex, EC (0.05-msec-long rectangular current pulses, 0.08–0.16 mA, one-sec-long trains with a 100 sec^{-1} frequency) in intact animals and rats after bilateral i.c.v. injections of $A\beta_{25–35}$ (from the next post-operational day). Stimulating and recording electrodes were inserted according to stereotaxic coordinates of the rat atlas [20] (EC: AP –10.0, L ±3.5, DV +4.0 mm; hippocampus: AP –3.5, L ± 1.5–3, DV +2.8–4.0 mm). Changes in the poststimulation activity were characterized as tetanic potentiation (TP) or tetanic depression (TD) followed by posttetanic potentiation (PTP) or depression (PTD).

Tissue Processing for Estimation of the Levels of Free Radicals. Mongrel albino rats i.c.v. injected with $A\beta_{25–35}$ and i.m. injected with ML venom or distilled water were decapitated. Then, samples of the liver, lung, heart, spleen, and kidney tissues were taken and homogenized for 5 min in Tris–HCl buffer (pH 7.4) with a final concentration of 20 mg/ml.

Chemiluminescence (ChL) Analysis. The levels of reactive oxygen species (ROSs) were measured by a highly sensitive ChL analyzing system; the intensities of luminescence of tissue homogenates were measured using a quantometric device, Junior LB 9509 portable tube luminometer (Berthold Technologies, Germany); the range of spectral sensitivity was 380 to 630 nm.

Lipid Peroxidation. Lipid peroxides are unstable; those are decomposed to a complex series of compounds among which the most abundant is malondialdehyde, MDA. The level of the latter in the tissues was measured using a spectrophotometric technique in the TBA test, based on the reaction of a chromogenic reagent, thiobarbituric acid (TBA), with MDA at 100°C. Two molecules of MDA reacting with one molecule of TBA produce a stable threemethin complex dye. The MDA concentration was measured at 532 nm using the CT-2600 spectrophotometer (CT-ChromTech, Taiwan).

Superoxide Dismutase (SOD) Activity. For the measurement of SOD activity, we used a method based on the ability of the enzyme to brake the reaction of autooxidation of adrenaline at pH 10.2. The adrenochrom concentration was measured at 480 nm using the above-mentioned CT-2600 spectrophotometer. The amount of the proteins was measured using the Lowry's method.

Statistical Analysis. For quantitative estimation of the chemiluminescence intensity, the Student's *t*-test was used to estimate intergroup differences between values at each time point, considering $P < 0.05$ as an index of significance. All numerical data are presented below as means ± s.e.m.; *n* is the number of experiments).

RESULTS

We examined the morphofunctional and electrophysiological characteristics of cellular structures of the rat hippocampus in intact animals, after bilateral i.c.v. injection of $A\beta_{25–35}$ amyloid, and after systemic administration of ML venom (in five experimental groups).

A laminated pattern in frontal hippocampal slices taken from intact rats (group 1) was quite obvious. Hippocampal pyramidal neurons were different in their size and shape and had noticeable branching processes. Large neurons were observed in the dentate gyrus (DG) and characterized by a high activity of phosphatase (Fig. 1C). Regularly arranged polygonal, triangular, and oval neurons were rather numerous in the *CA1* and *CA3* hippocampal areas; they were characterized by a high intensity of staining (Fig. 1A, a, B, b) [21].Their apical dendrites without branching could be traced at noticiable distances from the somata. The basal dendrites were clearly distinguished (Fig. 1A–C).

In the second experimental group (AD model), hippocampal neurons with surrounding glial elements in fields *CA1* and *CA3* were characterized by a sharp drop in phosphatase activity (Fig. 1D, E). The hippocampus of animals of this group demonstrated noticeable structural disorders. There was dramatic loss of pyramidal cells in the hippocampus along with neurofibrillary tangles; such a pattern is typical of AD neuropathology [22]. In neurons, their poles frequently

looked light, while other poles appeared strongly colored (Fig. 1D, E). Most intense degenerative changes were observed in the *CA1* field [23]. The shape and size of neurons were strongly distorted. In the neuronal processes, a spongy (alveolar) state of the cytoplasm was observed in both fields (*CA1* and *CA3*) (Fig. 1D, E). In the *CA1* area, there were "devastated" zones where neurons were absent; these zones bordered with zones of Gomori-positive granulation [24]. Glial cell were numerous in the DG and *CA3* field (Fig. 1E, F). The somata of neurons were going round; manifestations of swelling were observed in the *CA3*. In most neurons, chromatolysis was observed. In neurons, the nuclei usually occupied central positions (Fig. 1E). Large pyramidal cells in the DG possessed ectopic, disproportionally swallowed, and bloated nuclei surrounded by a dark layer. In these hippocampal regions, Gomori-positive granulation and senile plates were frequently present (Fig. 1F, f).

Rather interesting results were observed in AD rats treated with ML venom (group Aβ+venom). New nerve cells could be found in the devastated regions of the *CA1* field where enzymatic activity was low. The size and shape of neuronal units in all fields demonstrated signs of recovery. Nuclei of the cells were mostly localized in the centers of the latter; the cytoplasm

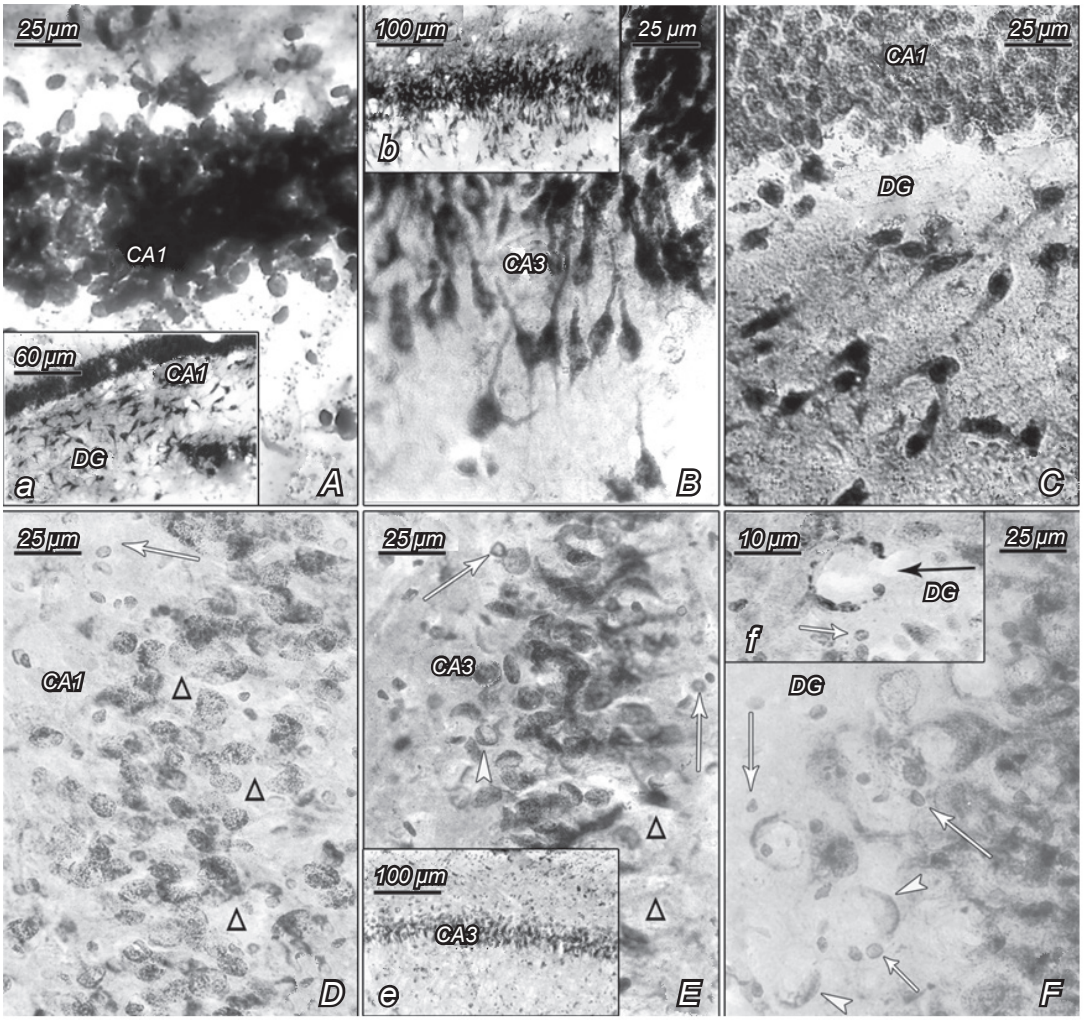

F i g. 1. Frontal slices of the hippocampus taken from intact rats (group 1, A–C) and rats after i.c.v. injection of amyloid $A\beta_{25–35}$ (group Aβ, D–F). Neurons localized in the *CA1* field (A, a, D), *CA3* field (B, b, E), and dentate gyrus (C, F, f). E, F) Central chromatolisys; black arrow) a senile plate; white arrow) core glia; triangle) a "devastated" area; arrowheads) ectopic nuclei of pyramidal neurons and central chromatolisys.

Р и с. 1. Фронтальні зрізи гіпокампа інтактних щурів (група 1, *A–C*) та щурів після інтрацеребровентрикулярної (i.c.v.) ін'єкції амілоїду $A\beta_{25–35}$ (група Aβ, *D–F*).

was filled with sediment grains and accumulations of granulation appeared around the pericaryons and processes. We believe that this pattern is typical of irritated neurons being on the road to recovery. (Fig. 2 A–C). The intensity of staining in neurons was rather variable. Throughout, blood microvessels with appendages (dendritic and somatic) were detected; this could be considered a manifestation of angiogenesis (Fig. 2a, b).

In the Aβ-affected rat brain, glial cells formed concentric rings around Aβ dense-cored plaques; this was generally found in close association with the plaques. Elements of microglia in these animals did not show dramatic morphological changes. This pattern may be related to the fact that microglial cells, in functional terms, are highly proinflammatory.

In rats i.c.v. injected with distilled water and i.m. injected with ML venom (group venom) an increase in the density of cells in all fields of the hippocampus was noticeable. There were no devastated regions in the hippocampus in such animals (Fig. 2D–F). Hippocampal neurons were hypertrophied compared with the analogous cells in the control (intact rats) [25]. At the same time, the shape of such units was rather similar to that observed in the control. These cells had normal-looking processes and laterally

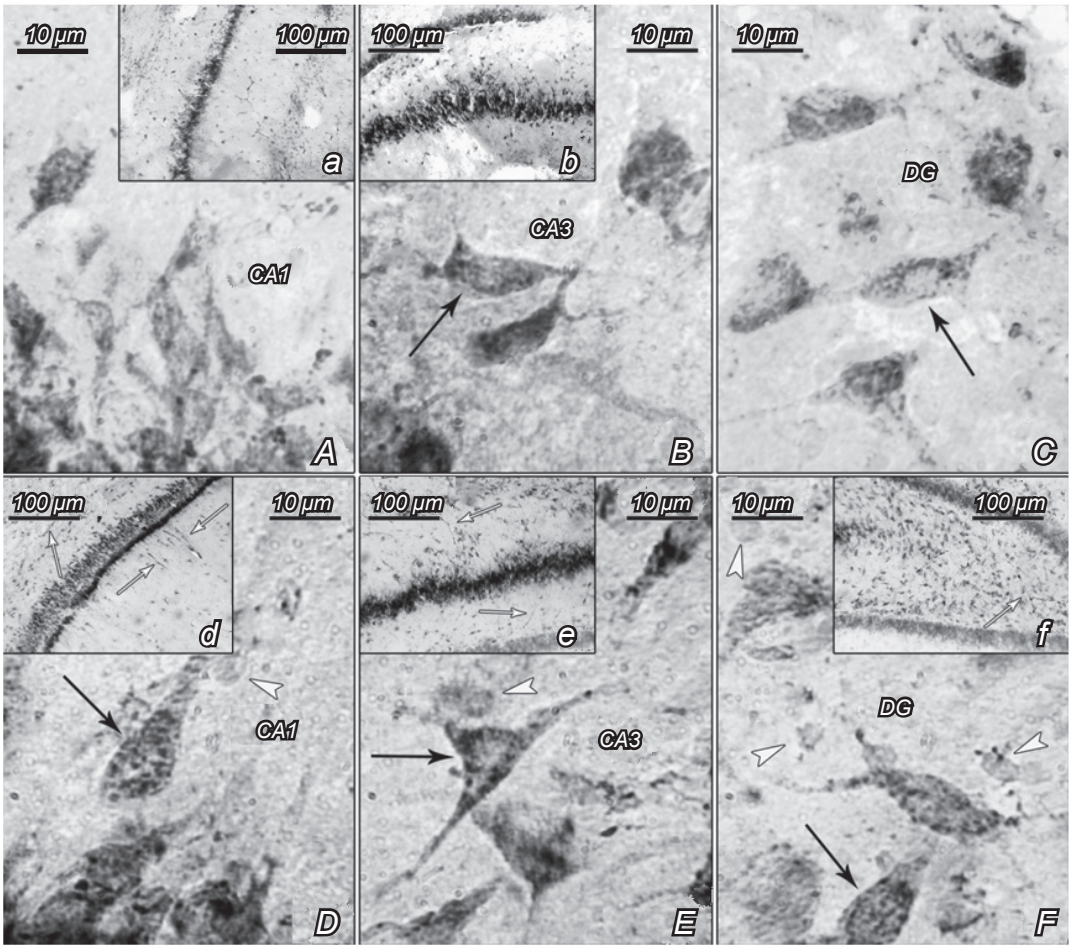

F i g. 2. Frontal slices of the hippocampus taken from rats i.c.v. injected with amyloid $A\beta_{25–35}$ and treated with i.m. injections of ML venom (group Aβ+venom, A–C) and rats injected i.c.v. with distilled water and i.m. with ML venom (group venom, D–F). Neurons in the *CA1* field (A, a, D, d), *CA3* field (B, b, E, e), and dentate gyrus, DG (C, F, f). Recovery of the normal morphology of neurons (A–C), the absence of "gaps" (a, b, d, f), a normal pattern of the apical and side dendrites (A–C), and hypertrophied cells with a high activity of acid phosphatase (D–F). Black arrow) Centrally located nucleus; white arrow) blood vessels with pericytes; arrowhead) core satellite glia.

Р и с. 2. Фронтальні зрізи гіпокампа після інтрацеребровентрикулярних (i.c.v.) ін'єкцій амілоїду $A\beta_{25–35}$ у щурів, котрим робили внутрішньом'язові (i.m.) ін'єкції отрути *Macrovipera lebetina* – ML, (група Aβ+отрута, *A–C*), та щурів, котрим i.c.v. ін'єкували дистильовану воду та i.m. – отруту ML (група «отрута», *D–F*).

extended dendrites (Fig. 2E, F). The apical dendrites of pyramidal neurons in the *CA1* and *CA3* fields were thickened (Fig. 2D). Gomori-positive granules in the cytoplasm (probably arising from degradation of the mitochondria and impaired mitochondrial oxidation of lipids) were found in all fields with a high enzymatic activity. This was the reason why such cells were intensely colored as compared with analogous cells in the control. The nuclei were localized in the centers of the cell somala. Neurons were surrounded with satellite glia, which can be interpreted as a sign of normal metabolic processes in the neural tissue. In most areas, blood vessels with pericytes were detected (angiogenesis) (Fig. 2 d–f) [26].

In Aβ-injected rats, many neurons of the hippocampus lost their characteristic shape in all fields. The contours of cells were frequently irregular and unclear; there were clear manifestations of central chromatolysis in a number of hippocampal cells of AD rats. The phosphatase activity in the nuclei of neurons was enhanced indicating certain activation of metabolism in the nucleus (Fig. 3A–C). In the *CA1* and *CA3* fields, certain zones were "devastated," and the territory around neurons looked empty (Fig. 3A, B). Many times, it was difficult to find the boundary between the body and protrusions of the neuron (Fig. 3A, B). Significant changes were also observed in DG pyramidal cells, while some neurons preserved

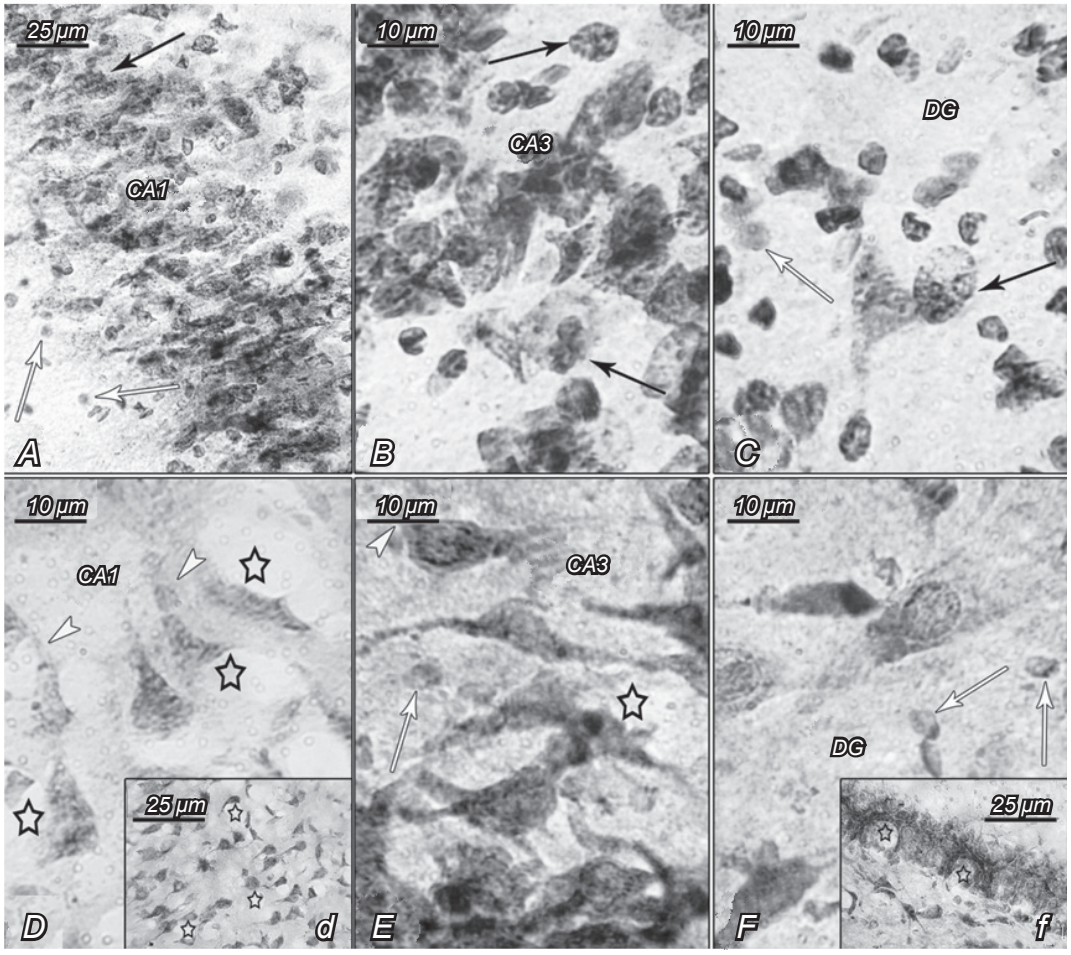

F i g. 3. Frontal slices of the hippocampus taken from rats i.c.v. injected with amyloid $A\beta_{25–35}$ (group Aβ, A–C) and rats injected i.c.v. and i.m. with distilled water (sham group, D–F, d–f). Neurons in the *CA1* field (A, a, D, d), *CA3* field (B, b, E), and dentate gyrus (C, F, f). A–C) Ectopic nuclei in hippocampal neurons, central chromatolisys; F) a decreased density of neurons in the DG granular layer;; black arrows) central chromatolisis; white arrow) nuclei of gliocytes; asterisks) manifestation of edema; arrowheads) thickened apical dendrites.

Р и с. 3. Фронтальні зрізи гіпокампа щурів після інтрацеребровентрикулярних (i.c.v.) ін'єкцій амілоїду $A\beta_{25–35}$ (група Aβ, *A–C*) та щурів, котрим i.c.v. та внутрішньом'язово (i.m.) ін'єкували дистильовану воду (контрольна група «псевдо», *D–F, d–f*).

normal morphology (Fig. 3C). We also observed single shapeless dark-colored formations morphologically resembling to pathological tau cells (Fig. 3B, C). Among shapeless degenerating neurons, the nuclei of glial cells could be distinguished clearly (Fig. 3 A–C). Clearly intensified extensive astrogliosis was another common feature observed in the brain of AD rats. It is well known that astrocytes are significantly modified in AD; in particular, they could be hypertrophied [27].

In rats i.c.v. injected with distilled water and i.m. injected also with water (sham group), noticeable morphological changes in the hippocampus usually were not observed; only in some cases we found swollen cells (Fig. 3D, F). The forms of the cells in the *CA1* and *CA3* fields and in the DG were practically identical to those in intact rats of group 1. Comparison of the morphological pattern in the hippocampus of Aβ-i.c.v. injected rats with that found in the sham group (Fig. 3) demonstrated that the AD model created in our study was rather adequate. Morphological changes, namely Gomori-positive granules with a high enzymatic activity in the cytoplasm of neurons, the presence of intensely colored cells (Fig. 3D, E), the presence of reactive satellite glia, and clear signs of intensified angiogenesis confirmed the above statement (Fig. 3D-F, d, f).

In electrophysiological recordings from rats of the AD (Aβ-i.c.v. injected) group 16 weeks after the above injections, the following balance of tetanic stimulation- related changes in spike activity of hippocampal neurons was observed. A TP-PTP sequence of poststimulation events was observed in 12.16 % of the cases; a TD-PTD pattern was found in 16.20%, a TD-PTP sequence was observed in 28.40%, while 43.24% of the cells showed no changes in their activity (i.e., were areactive). The Aβ+venom group demonstrated certain differences in stimulation-related changes in neuronal activity: TP-PTP, 12.35%; TD-PTD, 15.73%; TD-PTP, 61.00%, and 11.24% of neurons were areactive. In the venom group, the composition was the following: TP-PTP, 13.33%; TD-PTD, 33.33%, and TD-PTP-53.3%. In the sham group, the composition corresponded to the following figures: TP-PTP, 16.7%; TD-PTD, 41.70%, and TD-PTP, 41.7% (Fig. 4).

Thus, under the action of ML venom, the proportion of TD-PTP events increased from 42% to 54%, and TD-PTD decreased from 41% to 33%, as compared with the sham group. In the above groups, areactive units were practically absent, while the proportion of such neurons was rather significant in the Aβ group. Therefore, this fact is typical of the AD pathology. At the same time, when the action of ML venom was combined with that of Aβ amyloid, the share of areactive neurons became much smaller (11%); at the same time, the TD-PTP sequence was observed much more frequently (61%, compared with 28%) (Fig. 4).

In the next series of experiments, we investigated AD model-related changes in several body tissues except cerebral ones (hippocampus). It was found that, after injections of Aβ-amyloid, the intensity of free-radical activity characterized by chemoluminescence

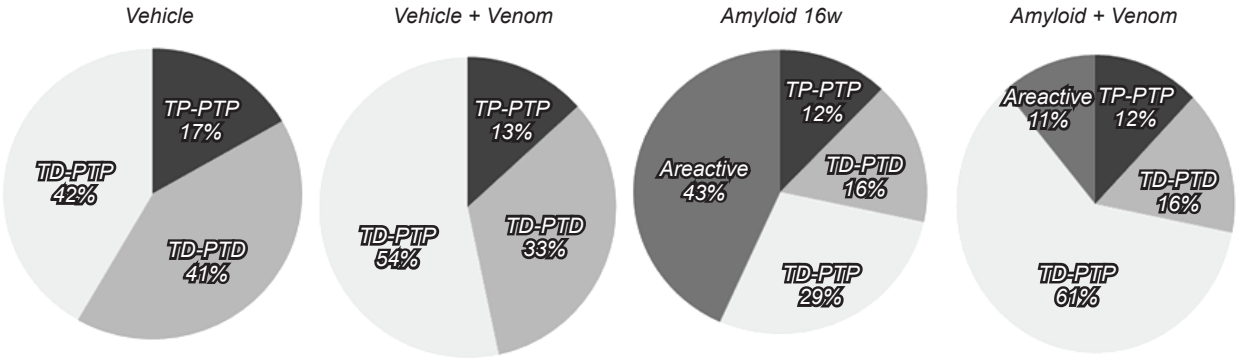

F i g. 4. Proportions, %, of types of changes in spike activity of hippocampal neurons induced by tetanic stimulation of the ipsilateral entorhinal cortex. Rats were i.c.v. and i.m injected with distilled water (A), i.c.v. with water and i.m. with ML venom (B), i.c.v. with amyloid $A\beta_{25–35}$ and i.m. with water (C), and i.c.v. with amyloid $A\beta_{25–35}$ and i.m. with ML venom (D). TP-PTP) Tetanic potentiation followed by posttetanic potentiation, TD-PTD) tetanic depression followed by posttetanic depression, TD-PTP) tetanic depression followed by posttetanic potentiation, and areactive) neurons that did not change their activity in the course and after stimulation.

Р и с. 4. Нормовані частоти (%) спостережуваних типів змін імпульсної активності, індукованих тетанічною стимуляцією іпсилатеральної енторинальної кори, в нейронах гіпокампа.

in the respective samples was significantly lower than in the control, in liver, lung, and heart tissues. Only in kidneys, this index was somewhat higher than in the norm. In most tissues, a combination of the action of Aβ with that of ML venom did not lead to restoration of free-radical processes and even increased the observed drops. Only in lung tissue, the effect of ML venom looked as some increase in the ChL intensity (Fig. 5).

The pattern of the observed changes was noticeably different when we measured the intensity of lipid peroxidation processes. In lung and heart tissues, this index characterized by the MDA concentration was significantly lower in Aβ-injected rats. In liver, this index practically did not changed, while in spleen and kidney tissues it was significantly higher than in the control (in kidney samples, more than two times). The effect of ML venom looked as an increase in the MDA concentration only in liver and heart tissues. In lung and spleen tissues, the effect was nearly negligible. At the same time, the effect of ML venom in kidney tissue looked as normalization of the described index (Fig. 6).

Since the analyzed lipid peroxidation processes in tissue are associated with the activity of the antioxidant enzyme systems, we, according to the same principle, measured the activity of superoxide dismutase (SOD), a first barrier in the antioxidant system. It was found that, in liver, lung, and spleen tissues the activity of the above enzyme was higher in Aβ-injected animals than in the control (in lung tissue, the increase was dramatic). At the same time, SOD activity in kidney tissues significantly dropped, while there were no significantly changes in the heart. In Aβ+ML venom-treated animals, the SOD activity returned to the values observed in the control, while in the heart and spleen, the action of ML venom induced significant increases in the activity of the examined enzyme. I kidney tissues, the effect of venom also looked as an increase, as compared with what was observed in the Aβ group, but the examined index did not reach the control values (Fig. 7).

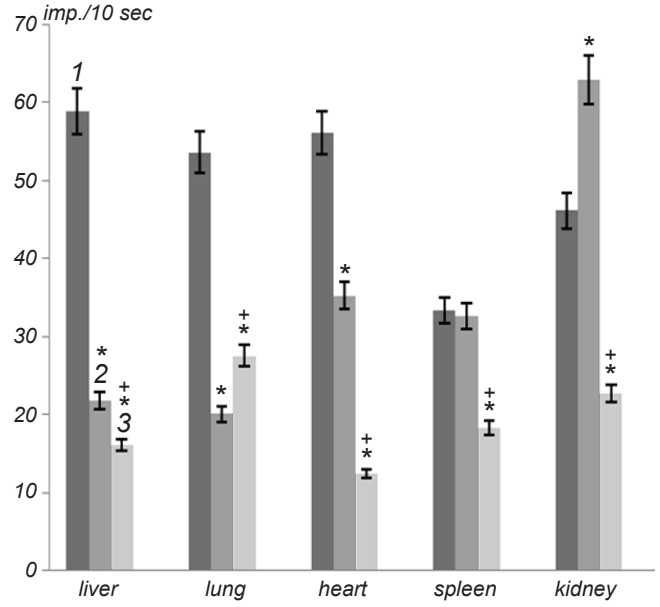

F i g. 5. Intensities of chemoluminescence, imp./10 sec, related to free radical activity in different tissues (shown below the diagrams) of control rats (1), rats after i.c.v. injection of amyloid $A\beta_{25–35}$ and i.m. injections of distilled water (2), and rats after i.c.v. injection of amyloid $A\beta_{25–35}$ treated with i.m. injections of ML venom (3). Cases of significant ($P < 0.05$) differences from values in the control group are shown by asterisks; significant differences between groups 2 and 3 are shown by plus-signs.

Р и с. 5. Значення інтенсивності хемолюмінесценції (кількості імпульсів у межах 10-секундних інтервалів), залежної від активності вільних радикалів у різних тканинах (вказані під діаграмами) контрольних щурів (*1*), щурів після інтрацеребровентрикулярних (i.c.v.) ін'єкцій амілоїду $A\beta_{25–35}$ та внутрішньом'язових (i.m.) ін'єкцій дистильованої води (*2*), а також щурів, котрим робили i.m.-ін'єкції отрути ML (*3*), після i.c.v.-ін'єкцій амілоїду $A\beta_{25–35}$.

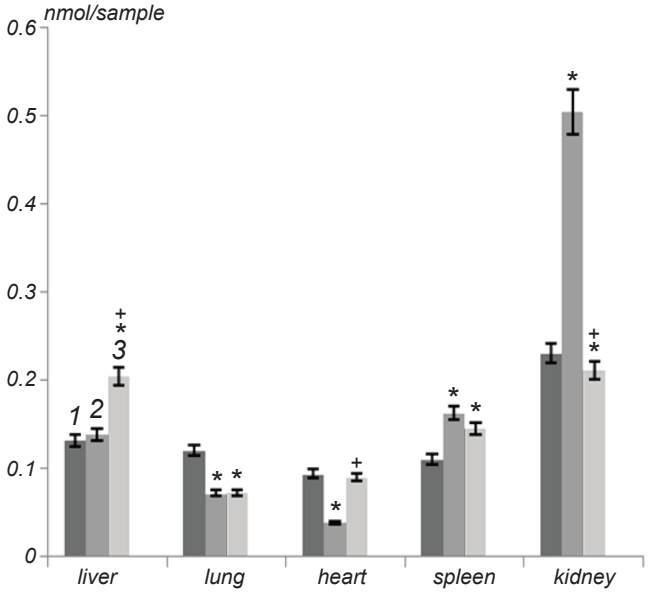

F i g. 6. Intensity of lipid peroxidation characterized by the malone dialdehyde concentration, nanomoles/assay, in different tissues of rats of the three groups. Designations are similar to those in Fig. 5.

Р и с. 6. Значення інтенсивності пероксидації ліпідів, виміряної як концентрація малонового діальдегіду (нмоль/зразок) у різних тканинах щурів трьох експериментальних груп

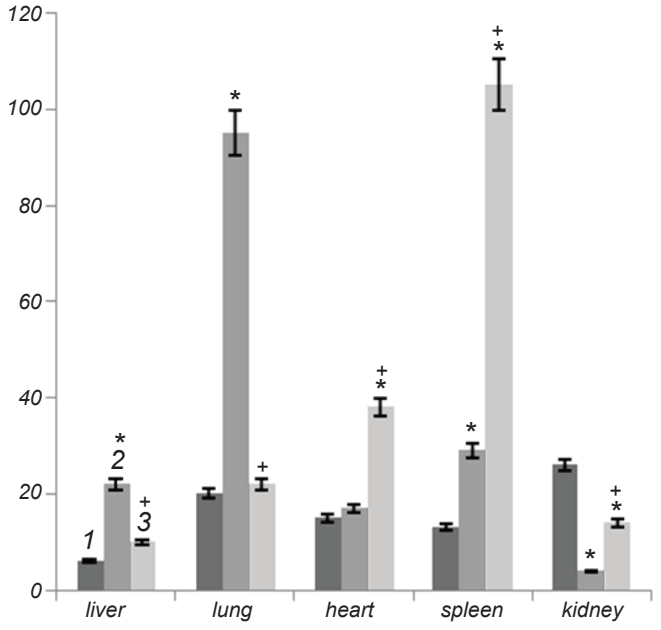

F i g. 7. Activity of superoxide dismutase (SOD), arb. units, in different tissues of rats of the three groups. Designations are similar to those in Figs. 5 and 6.

Р и с. 7. Значення активності супероксиддисмутази (SOD, умовні одиниці) у різних тканинах щурів трьох експериментальних груп.

DISCUSSION

Our main results can be summarized, most generally, in the following manner. Intracerebroventricular injections of Aβ peptide lead to significant negative changes in the morphology of hypothalamic structures, which mimicked those observed in AD. The action of ML venom results in noticeable restoration of the size and shape of hypothalamic cells (both neurons and gliocytes); it should be supposed that the action of low doses of this venom also provides restoration of the properties of the cell membranes. There were also considerable modifications of capillary-to-cell relations under conditions of the AD model. It is known that the vascular grows determines the intensity of cell proliferation and differentiation [28; it is believed that pericytes are derived from blood stromal cells [29]. The recovery of the size and shape of hypothalamic neurons may be interpreted as an adaptive response counteracting the development of neurofibrillary tangles [30]. Thus, the effect of the used doses of ML venom should be interpreted as a neuroprotective one. Positive changes in the structural properties of the neurons and restoration of the density of the neurons in the examined hippocampal fields were obvious; these changes may be related to restoration of cell metabolism, which determines better cell survival.

Excitatory effects observed under the influence of $A\beta_{25-35}$ peptide demonstrated a trend toward normalization after injections of small doses of ML venom. This fact is also indicative of an obvious neuroprotective action of the venom, irrespectively of the disease intensity in different rat models of AD. Within the framework of our AD model, mostly inhibitory stimulation-related effects of variable degrees were observed in hippocampal neurons. Within early stages of the AD development, the cognitive impairment associated with alterations of activities of the cholinergic and glutamatergic neuronal systems looks to be linked with decreases in the activity of cytosolic phospholipases A_2 and the activity of the arachidonic acid system [31]. Since phospholipases A_2 were shown to be implicated in the maintenance of neuronal homeostasis and memory formation, efforts to enhance the phospholipase A_2 activity may represent an important therapeutic approach in the AD treatment [32, 33]. Immunohistochemical studies demonstrated high levels of the expression of phospholipase A_2 in the hippocampus, cerebellum, and a few brainstem structures, with lower expressions in the thalamus and hypothalamus [34]. Recent experiments demonstrated a linkage between a phenomenon of adult neurogenesis and long-term synaptic plasticity in the dentate gyrus; this might provide new insites into the mechanisms by which interactions in the gene environment control the cognition and brain plasticity [35]. It is known that, during AD, degeneration of hippocampal glutamatergic and mesencephalic cholinergic neurons occurs; at the same time, GABA-ergic neurons remain relatively intact. It can be concluded that preservation of inhibition is a protective mechanism defending neurons in the course of AD [36].

Pathological manifestations of AD are degeneration of synaptic structures, deposition of amyloidal plaques, and that of neurofibrilary structures [37]. Oligomeric and protofibrillary forms of Aβ attack a wide spectrum of the neuronal and glial functions. These pathological structures are considered strong blockers of long-term potentiation (LTP), i.e., a form of synaptic plasticity responsible to significant structural changes in signaling pathways in neuronal networks. Under conditions of AD, dramatic disturbances of the synaptic mechanisms, particularly of manifestations of tetanic and posttetanic modifications, in the

hippocampus and entorhinal cortex were revealed [38]. Disorders of synaptic plasticity-related events, especially of those associated with LTP, represents the early functional alteration during AD [39].

As it became known at present, snake venoms, from a biochemical aspect, are complex mixtures of a pharmacologically active proteins and polypeptides. All of these components act in close interaction with each other, in concert. The synergistic action of venom proteins may enhance the activity or different venom components and contribute to rapid spreading of the toxins. Especially, the above-described synergy is important for venoms of the *Vipera* sub-family, because the compounds that could be identified as real toxins are practically absent in these venoms. The ML species and MLO subspecies belong to the *Vipera* sub-family, and venoms of these snakes contain different components that form complexes with other non-enzymatic proteins, to achieve a higher efficiency through synergy. It is known that MLO venom contains 14.6% of phospholipases A_2, and almost all enzymes of *Vipera*-like snakes are paralogs of the mammalian enzymes. Isolation of phospholipases A_2 from MLO venom and examination of the effects of these components in the AD model are the tasks of our future studies. Furthermore, it is also interesting for us to find a few components of the mentioned venom, which can act in a concert with phospholipase A_2 and enhance its neuroprotective abilities. It cannot be ruled out that such an approach would play a key role in the AD treatment. Therefore, these questions will be in the focus of our prospective studies; a combination of the above aspect with the experimental research of the effects of native venom should be considered quite expedient.

It should be mentioned that the data on SOD activity gave a nearly reverse image of the intensities of the free radical processes obtained by ChL analysis. This is quite expectable because it is known that the intensities of free radical processes and of the antioxidant system activity are strongly interdependent and responsible for the maintenance of a dynamic balance in the norm. Our results showed that there were some differences between the data of the TBA test and those of ChL analysis. This discrepancy is determined, as we suggest, by a methodological specificity of the TBA test. Results of the latter depend on the fact that only di- and polyunsaturated fatty acids and not monounsaturated ones are involved in the MDA formation. At the same time, such products as hydroperoxides of monounsaturated fatty acids significantly influence the level of ChL intensity in the respective measurements.

If we summarize our results, we can state that systemic administration of small doses of ML venom in the rat AD model induces positive changes in structural properties of hippocampal neurons, probably normalizes metabolism in this brain part, and intensifies the processes of Ca^{2+}-dependent phosphorylation. The density of neurons in the *CA1* and *CA2* fields and DG increases due to such ML venom treatment. This is indicative of certain moderation of negative effects induced by the action of $A\beta_{25–35}$ within the framework of the examined animal AD model.

Acknowledgment. This work was funded by the International Society for Neurochemistry (ISN Committee for Aid and Education in Neurochemistry, CAEN, category 1B; research supplies for the use in the applicant's home laboratory).

All experimental protocols were approved by the Committee of Ethics of the Yerevan State Medical University (YSMU, Yerevan, Armenia). All procedures were carried out in accordance with the European Communities Council Directive 2010/63/UE and documents of the local Animal Care Committee.

The authors of this communication, N. A. Ghazaryan, K. V. Simonyan, M. H. Danielyan, N. A. Zakaryan, L. A. Ghulikyan, G. R. Kirakosyan, V. A. Chavushyan, and N. M. Ayvazyan, confirm the absence of any conflict related to commercial or financial interests, to interrelations with organizations or persons in any way involved in the research, and to interrelations of the co-authors.

Н. А. Газарян[1], Л. М. Сімонян[1], М. Х. Даніелян[1], Н. А. Закарян[1], Л. А. Гюлікян[1], Г. Р. Кіракосян[1], В. А. Чавушян[1], Н. М. Айвазян[1]

НЕЙРОПРОТЕКТИВНІ ВПЛИВИ ОТРУТИ ГЮРЗИ (*MACROVIPERA LEBETINA*) В МОДЕЛІ ХВОРОБИ АЛЬЦГЕЙМЕРА

[1]Інститут фізіології ім. Л.А. Орбелі, НАН Республіки Вірменія, Єреван (Вірменія).

Р е з ю м е

Серед основних патологічних проявів при хворобі Альцгеймера (Alzheimer's disease, AD) називають накопичення та відкладання β-амілоїду (Aβ) у структурах мозку, активацію астроцитів і мікроглії та розлади холінергічної нейропередачі. У наших експериментах на щурах модель AD була відтворена за допомогою інтрацеребровентрикулярних

(і.ц.в.) ін'єкцій амілоїду $A\beta_{25–35}$. В іншій групі тварин це поєднувалось із внутрішньом'язовими (в.м.) ін'єкціями малих доз отрути гюрзи (*Macrovipera lebetina*, ML; 50 мкл 5 %-вого розчину дози LD_{50} на тварину, сім уведень з одноденними інтервалами). У тварин з моделюванням AD найбільш інтенсивно вражалися нейрони в полях гіпокампа *CA1* та *CA3*. Активність фосфатази в гіпокампі після ін'єкцій Аβ була значно зниженою. Системне введення малих доз отрути ML зумовлювало позитивні зміни структурних характеристик гіпокампальних нейронів, призводило до збільшення щільності нейронів у вказаних областях, нормалізувало метаболізм та інтенсифікувало кальційзалежні процеси фосфорилювання. Під дією отрути ML представленість відповідей пірамідних нейронів гіпокампа типу тетанічна депресія – посттетанічна потенціація в умовах високочастотної стимуляції іпсилатеральної енторинальної кори збільшувалася, спостерігалося також сумарне збільшення частоти імпульсації нейронів гіпокампа. Інтенсивність вільнорадикальних процесів у деяких тканинах щурів, котрим уводили Аβ, ставала значно меншою під дією отрути ML. Отже, ця отрута в малих дозах демонструє виражені нейропротективні впливи в умовах моделі хвороби Альцгеймера.

REFERENCES

1. F. Asadi, A. H. Jamshidi, F. Khodagholi, et al., "Reversal effects of crocin on amyloid β-induced memory deficit: Modification of autophagy or apoptosis markers," *Pharmacol. Biochem. Behav.*, **15**, 30083-30086 (2015).
2. J. H. Morrison and P. R. Hof, "Life and death of neurons in the aging cerebral cortex," *Int. Rev. Neurobiol.*, **81**, 41-57 (2007).
3. J. Shen and J. Wu, "Nicotinic cholinergic mechanisms in Alzheimer's disease," *Int. Rev. Neurobiol.*, **124**, 275-292 (2015).
4. J. M. Craft, D. M. Watterson, and L. J. Van Eldik, "Human amyloid β-induced neuroinflammation is an early event in neurodegeneration," *Glia*, **53**, 484-490 (2006).
5. E. Detrait, T. Maurice, E. Hanon, et al., "Lack of synaptic vesicle protein SV2B protects against amyloid-$\beta_{25–35}$-induced oxidative stress, cholinergic deficit and cognitive impairment in mice," *Behav. Brain Res.*, **271**, 277-285 (2014).
6. M. Pallas and A. Camins, "Molecular and biochemical features in Alzheimer's disease," *Current Pharm. Des.*, **12**, 4389-408 (2006).
7. M. Nagashima, S. Yasuhara, and J. A. Martyn, "Train-of-four and tetanic fade are not always a prejunctional phenomenon as evaluated by toxins having highly specific pre- and postjunctional actions," *Anesth. Analg.*, **116**, 994-1000 (2013).
8. P. Treppmann, I. Brunk, T. Afube, et al., "Neurotoxic phospholipases directly affect synaptic vesicle function," *J. Neurochem.*, **117**, 757-764 (2011).
9. R. Chen and S. E. Robinson, "The effect of cobrotoxin on cholinergic neurons in the mouse," *Life Sci.*, **51**, 1013-1019 (1992).
10. N. A. Ghazaryan, L. A. Ghulikyan, and N. M. Ayvazyan, "Morphological changes of proteolipid giant unilamellar vesicles affected by *Macrovipera lebetina obtusa* venom visualized with fluorescence microscope," *J. Membrane Biol.*, **246**, 627-632 (2013).
11. N. Vardjan, M. Mattiazzi, and E. Rowan, "Neurotoxic phospholipase A2 toxicity model: An insight from mammalian cells," *Commun. Integr. Biol.*, **6**, e23600 (2013).
12. N. A. Ghazaryan, L. Ghulikyan, A. Kishmiryan, et al., "Phospholipases A2 from *Viperidae* snakes: Differences in membranotropic activity between enzymatically active toxin and its inactive isoforms," *BBA-Biomembranes*, **1848**, 463-468 (2015).
13. L. Sanz, N. Ayvazyan, and J. J. Calvete, "Snake venomics of the Armenian mountain vipers *Macrovipera lebetina obtusa* and *Vipera raddei*," *J. Proteomics*, **71**, 198-209 (2008).
14. H. A. Bimonte-Nelson, A. C. Granholm, M. E. Nelson, and A. B. Moore, "Patterns of neurotrophin protein levels in male and female Fischer 344 rats from adulthood to senescence: how young is 'young' and how old is 'old'?" *Exp. Aging Res.*, **34**, 13-26 (2008).
15. T. Kurtovic, M. L. Balija, N. M. Ayvazyan, and B. Halassy, "Paraspecificity of *Vipera. ammodytes*-specific antivenom towards *Montivipera raddei* and *Macrovipera lebetina obtusa* venoms," *Toxicon*, **78**, 103-112 (2014).
16. T. Maurice, B. Lockhar, T. Su, and A. Privat, "Reversion of $\beta_{25–35}$-amyloid peptide-induced amnesia by NMDA receptor-associated glycine site agonists," *Brain Res.*, **731**, 249-253 (1996).
17. T. Maurice and A. Privat, "Sigma1 (sigma 1) receptor agonists and neurosteroids attenuate beta25–35-amyloid peptide-induced amnesia in mice through a common mechanism," *Neuroscience*, **83**, 413-428 (1998).
18. K. Yenkoyan, K. Safaryan, V. Chavushyan, et al., "Neuroprotective action of proline-rich polypeptide-1 in β-amyloid induced neurodegeneration in rats," *Brain Res. Bull.*, **86**, 262-271 (2011).
19. A. Chilingaryan, A. M. Chilingaryan, and G. G. Martin, "The three-dimensional detection of microvasculatory bed in the brain of white rat *Rattus norvegicus* by a Ca^{2+}-ATPase method," *Brain Res.*, **1070**, 131-138 (2006).
20. G. Paxinos and Ch. Watson, *The Rat Brain in Stereotaxic Coordinates*, Acad. Press, New York (2005).
21. L. Slomianka, T. Drenth, N. Cavegn, et al., "The hippocampus of the eastern rock sengi: cytoarchitecture, markers of neuronal function, principal cell numbers, and adult neurogenesis," *Front. Neuroanat.*, **29**, 34 (2013), doi: 10.3389/fnana.2013.00034.
22. D. M. Mann, "Pyramidal nerve cell loss in Alzheimer's disease," *Neurodegeneration*, **5**, 423-427 (1996).
23. T. C. Wen, J. Tanaka, H. Peng, et al., "Interleukin 3 prevents delayed neuronal death in the hippocampal *CA1* field," *J. Exp. Med.*, **188**, 635-649 (1998).
24. H. M. Schipper, D. E. Scarborough, R. M. Lechan, and S. Reichlin, "Gomori-positive astrocytes in primary culture: effects of *in vitro* age and cysteamine exposure," *Brain Res. Dev. Brain Res.*, **54**, 71-79 (1990).
25. K. Sugaya, M. Chouinard, R. Greene, et al., "Molecular indices of neuronal and glial plasticity in the hippocampal formation in a rodent model of age-induced spatial learning impairment," *J. Neurosci.*, **16**, 3427-3443 (1996).

26. G. Bergers and S. Song, "The role of pericytes in blood-vessel formation and maintenance," *Neurol. Oncol.*, **7**, 452-464 (2005).
27. W. Kamphuis, J. Middeldorp, and L. Kooijman, "Glial fibrillary acidic protein isoform expression in plaque related astrogliosis in Alzheimer's disease," *Neurobiol. Aging*, **35**, 492-510 (2014).
28. V. V. Banin, "Neoplasm of vessels: cellular and molecular mechanisms of regulation," *Morfologia (S. Petersburg), Materials of VI Congress of Int. Ass. of Morphologists, Kolos readings*, **18** (2002).
29. P. Bianco, M. Riminucci, S. Gronthos, and P. G. Robey, "Bone marrow stromal stem cells: nature, biology, and potential applications," *Stem Cells*, **19**,180-192 (2001).
30. M. Tolnay and F. Clavaguera, "Argyrophilic grain disease a late-onset dementia with distinctive features among tauopathies," *Neuropathology*, **24**, 269-283 (2004).
31. W. F. Gattaz, L. L. Talib, E. L. Schaeffer, et al., "Low platelet iPLA activity predicts conversion from mild cognitive impairment to Alzheimer's disease: a 4-year follow-up study," *J. Neural. Transm.*, **121**, 193-200 (2014).
32. L. L. Talib, S. R. Hototian, H. P. Joaquim, et al.,"Increased iPLA2 activity and levels of phosphorylated GSK3B in platelets are associated with donepezil treatment in Alzheimer's disease patients," *Eur. Arch. Psychiat. Clin. Neurosci.*, **265**, 701-706 (2015).
33. E. L. Schaeffer, O. V. Forlenza, and W. F. Gattaz, "Phospholipase A(2) activation as a therapeutic approach for cognitive enhancement in early-stage Alzheimer disease," *Psychopharmacology*, **202**, 37-51 (2009).
34. Y. Shirai and M. Ito, "Specific differential expression of phospholipase A2 subtypes in rat cerebellum," *J. Neurocytol.*, **33**, 297-307(2004).
35. B. Lu and J. H. Chang, "Regulation of neurogenesis by neurotrophins: implications in hippocampus dependent memory," *Neuron Glia Biol.*, **1**, 377-384 (2005).
36. D. A. Nation, C. E. Wierenga, L. R. Clark, et al., "Cortical and subcortical cerebrovascular resistance index in mild cognitive impairment and Alzheimer's disease," *J. Alzheimers Dis.*, **36**, 689-698 (2013).
37. J. H. Birnbaum, J. Bali, L. Rajendran, et al., "Calcium flux-independent NMDA receptor activity is required for Aβ oligomer-induced synaptic loss," *Cell Death Dis.*, **18**, e1791 (2015), doi: 10.1038/cddis.2015.160.
38. M. P. Mattson and S. L. Chan, "Neuronal and glial calcium signaling in Alzheimer's disease," *Cell Calcium*, **34**, 385-397 (2003).
39. J. Gocel and J. Larson, "Synaptic NMDA receptor-mediated currents in anterior piriform cortex are reduced in the adult fragile X mouse," *Neuroscience*, **221**, 170-181 (2012).